Conference papers

School of Mathematics and Statistics

Numerical Modeling of Weakly Ionized Plasmas

Stephen O'Sullivan
Technological University Dublin, stephen.osullivan@tudublin.ie

Turlough Downes
Dublin City University

Numerical modeling of weakly ionized plasmas.

Stephen O'Sullivan

UCD School of Mathematical Sciences, University College Dublin, Dublin 4, Ireland

Turlough P. Downes

School of Mathematical Sciences, Dublin City University, Glasnevin, Dublin 9, Ireland
National Centre for Plasma Science and Technology, Dublin City University, Glasnevin, Dublin 9, Ireland

Abstract.
Multifluid magnetohydrodynamics is not a well explored field of numerical astrophysics. The reasons for this have been largely pragmatic due to the inherent difficulties of applying conventional numerical methods; explicit techniques range in efficiency from low to none, and implicit techniques are notoriously problematic for codes which rely on distributed architectures and adaptive mesh refinement (AMR) as is *de rigeur* for modern large scale simulations.

In this paper, a novel explicit technique is presented which does not suffer the same strong efficiency constraints as conventional explicit methods. The symmetric and skew-symmetric components of the multifluid diffusion operator are multiplicatively operator split and integrated via an accelerated substepping scheme, and an unconditionally stable explicit method respectively. Crucially, unlike implicit methods, the technique is also easily implemented in existing AMR driven and parallelised code frameworks.

1. Introduction

In a weakly ionized plasma the bulk mass of the gas is in the neutral component. Under conditions typical of many astrophysical environments the pressure and inertia of the charged species in the gas may be neglected. In order to expedite the discussion of the numerical method, we assume an isothermal three-fluid plasma, with no mass transfer between species. These restrictions are easily relaxed as described in (O'Sullivan & Downes 2006, 2007, hereafter OSD06 and OSD07 respectively).

The importance of magnetic forces on each charged species, relative to collisional drag on the neutral gas, is parametrized by the Hall parameter $\beta_z \equiv \frac{\alpha_z B}{K_z \rho_n}$, where the subscripts n, e, i indicate properties relating to the neutral gas, electrons, and ions respectively and z represents the charged species index e or i. α_z are the charge-to-mass ratios and and K_z are the collisional coefficient with respect to the neutral gas of charged species z.

The diffusion of the magnetic field through the bulk plasma may occur in one of three different regimes according to the relative magnitudes of the Hall

1

parameters: $\beta_i \ll |\beta_e| \ll 1$ indicates the Ohmic regime where the charged species are decoupled from the magnetic field; $1 \ll \beta_i \ll |\beta_e|$ corresponds to the ambipolar regime where the charged species are tightly coupled to the field; and $\beta_i \ll 1 \ll |\beta_e|$ describes the Hall regime where the electrons are tied to the field lines but the ions are not.

In protostellar disks, for example, Wardle (2007) concludes that each of these regimes may be present itself. It is therefore crucial to our understanding of star and planet formation to properly treat multifluid processes in weakly ionized plasmas. Problematically, it has been pointed out that conventional explicit techniques are inappropriate in treating such systems (Falle 2003, hereafter F03).

2. Multifluid equations

The equations governing a three-fluid isothermal plasma are

$$\frac{\partial \rho_x}{\partial t} + \nabla \cdot (\rho_x \boldsymbol{q}_x) = 0, \tag{1}$$

$$\frac{\partial \rho_n \boldsymbol{q}_n}{\partial t} + \nabla \cdot \left(\rho_n \boldsymbol{q}_n \boldsymbol{q}_n + a^2 \rho_n \mathsf{I} \right) = \boldsymbol{J} \times \boldsymbol{B}, \tag{2}$$

$$\alpha_z \rho_z \left(\boldsymbol{E} + \boldsymbol{q}_z \times \boldsymbol{B} \right) + \rho_z \rho_n K_z (\boldsymbol{q}_n - \boldsymbol{q}_z) = 0, \tag{3}$$

$$\frac{\partial \boldsymbol{B}}{\partial t} + \nabla \cdot (\boldsymbol{q}_n \boldsymbol{B} - \boldsymbol{B} \boldsymbol{q}_n) = -\nabla \times \boldsymbol{E}', \tag{4}$$

where physical quantities are represented by the usual symbols and x is one of n, e, i and

$$\boldsymbol{E}' = \boldsymbol{E} + \boldsymbol{q}_n \times \boldsymbol{B} = r_{\mathrm{O}} \boldsymbol{J}_{\parallel} + r_{\mathrm{H}} \boldsymbol{J}_{\perp} \times \hat{\boldsymbol{B}} + r_{\mathrm{A}} \boldsymbol{J}_{\perp} \tag{5}$$

is the electric field in the local rest frame of the bulk plasma and a is the isothermal soundspeed.

The Ohmic (field parallel), Hall and ambipolar (Pedersen) resistivities are given by

$$r_O = \frac{1}{\sigma_O}, \quad r_H = \frac{\sigma_H}{\sigma_H^2 + \sigma_A^2}, \quad r_A = \frac{\sigma_A}{\sigma_H^2 + \sigma_A^2}, \tag{6}$$

with related conductivities

$$\sigma_O = \sum_{i=2}^{N} \alpha_i \rho_i \beta_i, \quad \sigma_H = \frac{1}{B} \sum_{i=2}^{N} \frac{\alpha_i \rho_i}{1 + \beta_i^2}, \quad \sigma_A = \frac{1}{B} \sum_{i=2}^{N} \frac{\alpha_i \rho_i \beta_i}{1 + \beta_i^2}. \tag{7}$$

Finally, conditions for a solenoidal field, and charge and current neutrality are enforced via

$$\nabla \cdot \boldsymbol{B} = 0, \quad \sum_{i=2}^{N} \alpha_i \rho_i = 0, \quad \sum_{i=2}^{N} \alpha_i \rho_i \boldsymbol{q}_i = \boldsymbol{J}. \tag{8}$$

3. Numerical method

To obtain the full solution at time $t + \tau$, standard finite volume integration methods are applied to hyperbolic and source terms in the governing equations of the neutral gas. The time integration is multiplicatively operator split with each operation carried out to second order accuracy and Richardson extrapolation invoked for second order temporal accuracy. For further details the reader is referred to F03, SD06, SD07.

We now consider exclusively the $\nabla \times \boldsymbol{E}'$ term on the right hand side of equation 4 and assume the Ohmic resistivity is negligible (which is often a reasonable assumption but does not present significant difficulties otherwise). Then, making the definitions $\boldsymbol{a}_\mathrm{O} \equiv \sqrt{r_\mathrm{O}}\boldsymbol{b}$, $\boldsymbol{a}_\mathrm{H} \equiv r_\mathrm{H}\boldsymbol{b}$, $\boldsymbol{a}_\mathrm{A} \equiv \sqrt{r_\mathrm{A}}\boldsymbol{b}$ where $\boldsymbol{b} \equiv \boldsymbol{B}/B$, and discarding higher order terms reduces equation 4 to

$$\partial \boldsymbol{B}/\partial t = (\boldsymbol{a}_\mathrm{H} \cdot \nabla)\boldsymbol{J} + [\boldsymbol{a}_\mathrm{A} \cdot (\nabla \times \boldsymbol{J})]\boldsymbol{a}_\mathrm{A} - [(\boldsymbol{a}_\mathrm{A} \cdot \nabla)\boldsymbol{J})] \times \boldsymbol{a}_\mathrm{A}. \tag{9}$$

In order to examine the stability properties of explicit discretizations of equation 9 we consider a numerical wave of the form $\boldsymbol{B}^l_{ijk} = \boldsymbol{B}_0\exp[\mathrm{i}\,(i\omega_x + j\omega_y + k\omega_z)]$ where l is the time index of the solution and i, j, k, are the x, y, z spatial indices. This permits substitutions for simple centred difference approximations to the second order spatial derivatives in equation 9 according to $\partial^2/\partial x^2 \to \Lambda_{xx} \equiv -2(1-\cos\omega_x)$, $\partial^2/\partial x\,\partial y \to \Lambda_{xy} \equiv -\sin\omega_x \sin\omega_y$, and similar expressions for the other terms yielding

$$\boldsymbol{B}^{l+1} = (\mathbf{I} - \alpha r_\mathrm{H}\mathbf{A}_\mathrm{H} - \alpha r_\mathrm{A}\mathbf{A}_\mathrm{A})\boldsymbol{B}^l \tag{10}$$

where $\alpha = \tau/h^2$, $\mathbf{A}_\mathrm{A} = \mathbf{b}\boldsymbol{\zeta}+\boldsymbol{\zeta}\mathbf{b}-\mathrm{tr}(\Lambda)\mathbf{b}\mathbf{b}-\boldsymbol{b}^T\boldsymbol{\zeta}\mathbf{I}$, and $\mathbf{A}_\mathrm{H} = \begin{pmatrix} 0 & \zeta_z & -\zeta_y \\ -\zeta_z & 0 & \zeta_x \\ \zeta_y & -\zeta_x & 0 \end{pmatrix}$

with $\boldsymbol{\zeta} \equiv \Lambda\boldsymbol{b}$ and $\boldsymbol{b} \equiv \boldsymbol{B}/B$.

In the limiting case of $\mathbf{A}_\mathrm{H} = 0$, we find the eigenvalues of the corresponding amplification matrix $(\mathbf{I} - \alpha r_\mathrm{A}\mathbf{A}_\mathrm{A})$ are $\mu_1 = 1 + \alpha r_\mathrm{A}\boldsymbol{b}^T\boldsymbol{\zeta}$ and $\mu_{2,3} = 1 + \frac{1}{2}\alpha r_\mathrm{A}[\mathrm{tr}(\Lambda) \pm |\mathrm{tr}(\Lambda)\boldsymbol{b} - 2\boldsymbol{\zeta}|]$. The spectral radius of the evolution operator is then determined by considering $\boldsymbol{\omega} = \pi(1,\,1,\,1)$ for arbitrary $\boldsymbol{b}$. We find

$$\bar{\tau} \le \frac{1}{2}\frac{\sqrt{1+\eta^2}}{\eta} \qquad \text{for} \qquad \mathbf{A}_\mathrm{H} = 0 \tag{11}$$

where $\bar{\tau} \equiv \tau/\tau^\perp$, $\tau^\perp = \frac{h^2}{2\sqrt{r_\mathrm{H}^2+r_\mathrm{A}^2}}$, and $\eta \equiv r_\mathrm{A}/|r_\mathrm{H}|$. While this timestep goes as h^2 as expected, the integration of symmetric operators can be accelerated via Super TimeStepping (STS) (Alexiades, Amiez & Gremaud 1996, OSD06, OSD07).

On the other hand, when $\mathbf{A}_\mathrm{A} = 0$, $(\mathbf{I} - \alpha r_\mathrm{A}\mathbf{A}_\mathrm{H})$ is unstable (F03, OSD06, OSD07). Therefore, conventional explicit methods are inappropriate for problems for which there is a large Hall term. We circumvent this limitation without resorting to implicit methods by a component-wise multiplicative operator splitting of $(\mathbf{I} - \alpha r_\mathrm{A}\mathbf{A}_\mathrm{H})$ in an exploit of its skew-symmetry which we call the Hall Diffusion Scheme (HDS) (see OSD07 for further details). The alternate evolution operator, $(\mathbf{I} - \alpha r_\mathrm{H}\mathbf{kk}\mathbf{A}_\mathrm{H})(\mathbf{I} - \alpha r_\mathrm{H}\mathbf{jj}\mathbf{A}_\mathrm{H})(\mathbf{I} - \alpha r_\mathrm{H}\mathbf{ii}\mathbf{A}_\mathrm{H})$, has a finite spectral radius

dictated by a maximum magnitude eigenvalue found at $\boldsymbol{\omega} = (2\pi/3)(1, 1, 1)$ with $\boldsymbol{b} = (1/\sqrt{3})(1, 1, 1)$. We find

$$\bar{\tau} \leq \frac{4}{\sqrt{27}}\sqrt{1 + \eta^2} \qquad (12)$$

.

Our strategy in general therfore is to multiplicatively operator split the diffusion operator into symmetric and skew symmetric components and handle these respectively via STS and HDS techniques.

4.   Results

4.1.   Oblique shock tube test

We present three one-dimensional shock tube tests oriented obliquely to the coordinate axes. In each case the test is set up along the $(1, 1, 1)$ direction in a narrow channel on a cubic mesh with appropriate boundary conditions assigned to cells outside the channel (see OSD07 for further details).

Case A: Ambipolar regime ($r_O = 2 \times 10^{-12}$, $r_H = 1.16 \times 10^{-5}$, $r_A = 0.068$, $\eta = 5.86 \times 10^3$)

R:	$\rho_n = 1$	$\boldsymbol{q}_n = (-1.751, 0, 0)$	$\boldsymbol{B} = (1, 0.6, 0)$	$\rho_e = 5 \times 10^{-8}$	$\rho_i = 1 \times 10^{-3}$
L:	$\rho_n = 1.79$	$\boldsymbol{q}_n = (-0.976, -0.656, 0)$	$\boldsymbol{B} = (1, 1.75, 0)$	$\rho_e = 8.97 \times 10^{-8}$	$\rho_i = 1.79 \times 10^{-3}$
	$\alpha_e = -2 \times 10^{12}$	$\alpha_i = 1 \times 10^8$	$K_e = 4 \times 10^5$	$K_i = 2 \times 10^4$	$a = 0.1$
	$\nu = 0.05$	$N_{\text{STS}} = 5$	$N_{\text{HDS}} = 0$		

Case B: Hall regime ($r_O = 2 \times 10^{-9}$, $r_H = 0.0116$, $r_A = 5.44 \times 10^{-4}$, $\eta = 0.046 \ll 1$)

R:	As case A				
L:	As case A				
	$\alpha_e = -2 \times 10^9$	$\alpha_i = 1 \times 10^5$	$K_e = 4 \times 10^2$	$K_i = 2.5 \times 10^6$	$a = 0.1$
	$\nu = 0$	$N_{\text{STS}} = 1$	$N_{\text{HDS}} = 8$		

Case C: Neutral subshock (resistivities as in Case A)

R:	$\rho_n = 1$	$\boldsymbol{q}_n = (-6.72, 0, 0)$	$\boldsymbol{B} = (1, 0.6, 0)$	$\rho_e = 5 \times 10^{-8}$	$\rho_i = 1 \times 10^{-3}$
L:	$\rho_n = 10.4$	$\boldsymbol{q}_n = (-0.645, -1.09, 0)$	$\boldsymbol{B} = (1, 7.95, 0)$	$\rho_e = 5.21 \times 10^{-7}$	$\rho_i = 1.04 \times 10^{-2}$
	$\alpha_e = -2 \times 10^{12}$	$\alpha_i = 1 \times 10^8$	$K_e = 4 \times 10^5$	$K_i = 2 \times 10^4$	$a = 1$
	$\nu = 0.05$	$N_{\text{STS}} = 15$	$N_{\text{HDS}} = 0$		

Table 1.   Shock tube test parameters. Right and left state values are denoted R and L.

In each test, with initial conditions described in Table 1, the solution obtained using the dynamic code is compared with solutions obtained via the analytical steady-state solutions. In all cases the agreement between the solutions is good as can be seen in Figure 1. Cases A and B are found to have convergence rates close to second order as expected for smooth solutions. The subshock in the neutral flow of case C is clearly visible as a discontinuity in u_n, while there is no corresponding discontinuity in B_y. As a result of the discontinuity, the convergence is at first order.

4.2.   Unforced and forced turbulence.

In this section, we briefly outline two additional tests of the numerical techniques described here and refer to the reader to OSD07, and Tanner, O'Sullivan &
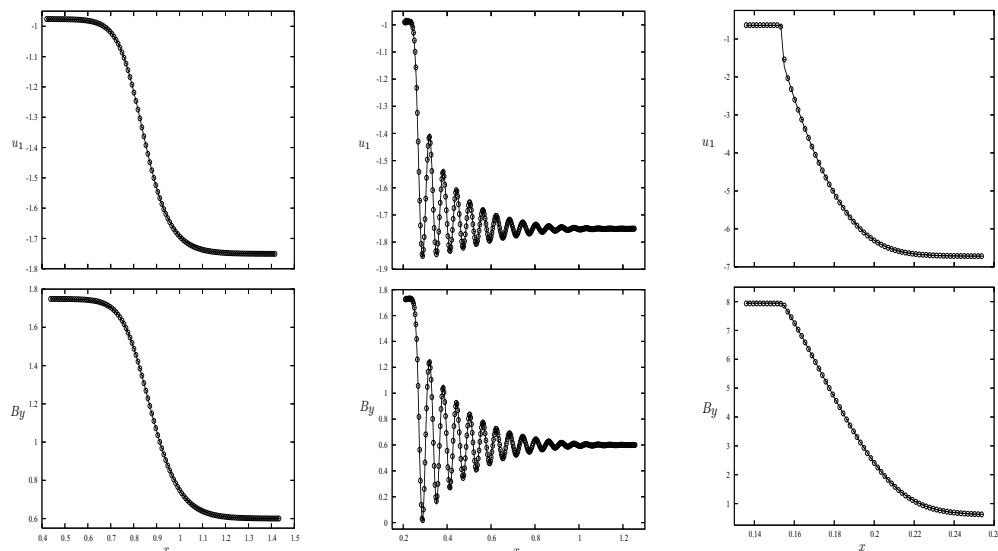
Figure 1.   Neutral fluid x-velocity (top) and y-component of magnetic field (bottom) for oblique shock tube test cases A (left), B (middle), and C (right). The steady state solution is shown as a line.

Downes (in prep.) for a more complete description. In each case, the behaviour of a turbulent magnetic field in a three-dimensional volume of a three-fluid weakly ionized isothermal plasma is examined under different multifluid regimes.

In the first instance the turbulence is imposed as an initial condition under ambipolar and Hall regimes. The left panel of Fig. 2 shows the density power spectra of the initially uniform gas after 5 sound crossing times. Clearly there is far more structure at all scales for the Hall case (except for some low power grid-scale noise at high frequencies). This behaviour should have significant consequences for any gravitationally unstable system. Note that, in a related study, turbulent decay under the Hall effect is considered by Downes & O'Sullivan (this volume).

In a second test, the turbulence is driven by impulses from randomly generated helical forcing modes (Brandenburg 2001) in Ohmic, ambipolar, and Hall regimes. Dynamo action is observed as the initially small seed field is pumped up to equipartition values with the kinetic energy where it saturates. Significantly, as seen in the right panel of Fig. 2, the saturation levels of the magnetic energy for each of the cases are different.

5.   Conclusions

We have presented a method for treating diffusion of the magnetic field in a weakly ionized plasma through explicit techniques. The diffusion operator is multiplicatively split into its symmetric and skew-symmetric components and integrated via STS and HDS respectively. The resultant stability properties are superior to conventional explicit techniques without requiring the complexity
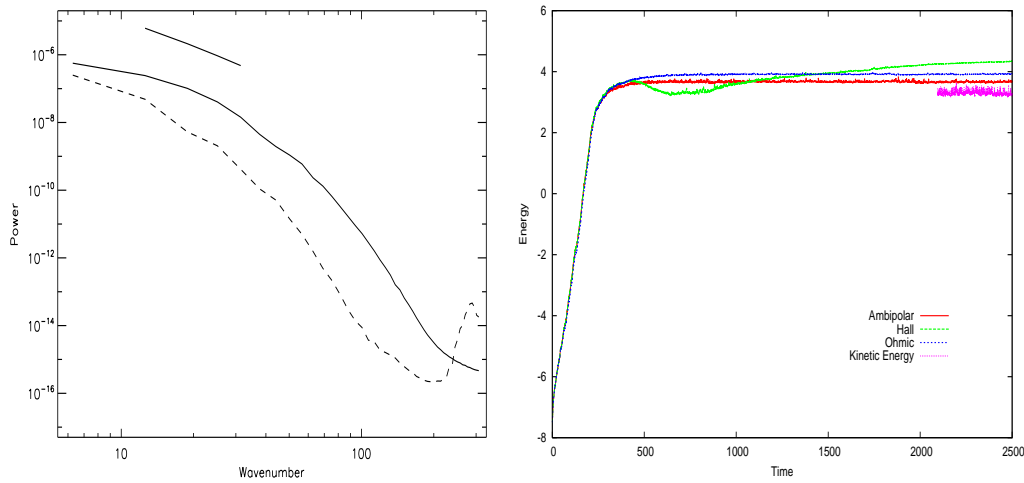
Figure 2.   Left panel: Density power spectra for Hall (solid line) and ambipolar (dashed line) unforced turbulence test cases. A Kolmogorov power law (solid straight line) is also shown for reference. Right panel: Magnetic energy against time for random forcing turbulent dynamo in three different multifluid regimes.

of implicit methods. Implementation in conjunction with distributed domain decomposition and adaptive mesh refinement is trivial.

Finally, we have described results of shock-tube tests, and forced and unforced turbulence problems which demonstrate the accuracy and efficacy of the methods presented here.

References

Alexiades V., Amiez G., Gremaud P., 1996, Com. Num. Meth. Eng., 12, 31
Brandenburg A., 2001, ApJ., 550, 824
Ciolek G.E., Roberge, W.G., 2002, ApJ, 567, 947
Falle S.A.E.G., 2003, MNRAS, 344, 1210 (F03)
O'Sullivan S., Downes T.P., 2006, MNRAS, 366, 1329 (OSD06)
O'Sullivan S., Downes T.P., 2007, MNRAS, 376, 1648 (OSD07)
Tanner S.E.M., O'Sullivan S., Downes T.P, in prep.
Wardle M., 2007, Astrophys. Space Sci., online
Wardle M., Ng C., 1999, MNRAS, 303, 239